EXTENDED MODEL EQUATION FOR UNCOVERED COLLECTORS

Klaus Vajen, Marcel Krämer[#], Elimar Frank
Universität Kassel, Institut für Thermische Energietechnik, D–34109 Kassel, Germany
phone +49/561/804-3891, fax +49/561/804-3993, solar@uni-kassel.de

Erkin K. Boronbaev
Kyrgyz State University of Construction, Transportation and Architecture, KS-720023 Bishkek Kyrgyzstan

Ralf Orths
Wagner&Co Solartechnik, D-35091 Cölbe, Germany

Abstract A test system with 50 m² uncovered collector was installed and operated connected to a district heating net in Bishkek (Kyrgyzstan). The useful power gain as well as the weather conditions were measured for two months with a high time resolution. The collector was driven with water inlet temperatures far below the ambient temperature level. For the description of the energy balance of the collector an extension of the customary model equations was necessary. The extended model equation consider different heat transfer mechanisms and coefficients which are effective on different and varying sections of the absorber at the same time and includes e.g. convective and condensation heat transfer. The results of the model are compared with measured data. If the boundary conditions, especially the time series of weather, are known, with the model proper long term predictions can be carried out regarding the expected collector gain even for unusual conditions as described above.

1. INTRODUCTION

Numerical models are used to describe the thermal behaviour of solar collectors. If the parameters of the model are theoretically or experimentally determined, the model should deliver the thermal power gained by the collector for given boundary conditions like weather, fluid inlet temperature and mass flow. For uncovered collectors one node models, consisting of a single equation, are described in literature (EN 12795, ISO 9806). As an example, EN 12795 (2001 without the corrections AC 2002) stipulates the usage of the following equation:

$$\dot{q}_{use} = F' \cdot K_{\alpha,b} \cdot \alpha_\perp \cdot G_{bT} + F' \cdot K_{\alpha,d} \cdot \alpha_\perp \cdot G_{dT}$$
$$- c_6 \cdot v_w \cdot G_T - c_1 \cdot (T_f - T_a)$$
$$- c_2 \cdot (T_f - T_a)^2 - c_3 \cdot v_w \cdot (T_f - T_a) \tag{1}$$
$$+ c_4 \cdot (E_L - \sigma T_a^4) - c_5 \cdot dT_f / dt$$

These models cover the standard operation temperatures and do not include e.g. heat gains due to condensation. Furthermore, it is assumed that the heat transfer coefficient is constant for the entire collector. Implicitly a specific arrangement of the temperatures is assumed:

$$T_d < T_a < T_i < T_o . \tag{2}$$

For some applications, e.g. (Vajen et al 1999), the fluid inlet temperature can be predominantly lower than the ambient temperature and for special boundary conditions even below the dew point temperature. In these cases condensation of the air humidity takes place at least on a part of the collector. Again depending on the constraints, the fluid outlet temperature may be lower or higher than the ambient temperature. This can lead to convective heat gains on that part of the collector close to the fluid inlet and heat losses close to the outlet. The models known so far were not able to describe the thermal behaviour of collectors properly which are operated that way. Therefore an extended model equation was developed.

2. EXTENDED MODEL EQUATION

As for eq. (1), one model assumption is an even flow through all absorber channels connected in parallel. Additionally, heat transport in flow direction takes only place by the fluid flow and not e.g. by conduction. This assumption applies to absorbers made of rubber or plastic, but also for most of the metal absorbers. The difference of the upper absorber surface and the corresponding fluid temperature is assumed to be independent of the position in fluid flow direction. Furthermore, between fluid inlet and outlet a linear increase of the temperatures of fluid and absorber surface is assumed. Thus, the validity of the models is limited to sufficiently high specific flow rates. All heat capacities are lumped together in a single node, represented by the average fluid temperature. The heat transfer is modelled quasi-stationary and the heat transfer coefficients are assumed to be constant for the specific absorber ranges and time intervals looked at.

Following an approach of (Perers 1987) the energy balance at the absorber surface is the starting point of the considerations.

[#] present address: deneg, D-28211 Bremen

$$\dot{q}_{use} + \dot{q}_b + c_{eff} \cdot \frac{dT_f}{dt} = h_i \cdot \left(T_p - T_f\right) \tag{3}$$

$$= \dot{q}_{abs} - \dot{q}_{sky} - \dot{q}_{conv} - \dot{q}_{cond}$$

with

$$\dot{q}_{use} = \dot{v}\, c_p\, \rho \left(T_o - T_i\right) \tag{4}$$

$$\dot{q}_b = U_b \left(T_f - T_a\right) \tag{5}$$

$$T_f = \left(T_o + T_i\right)/2 \tag{6}$$

$$\dot{q}_{abs} = K_{\alpha,b}\!\left(\theta, \gamma'_s\right) \cdot \alpha_\perp \cdot G_{bT} + K_{\alpha,d} \cdot \alpha_\perp \cdot G_{dT} \tag{7}$$

$$\dot{q}_{sky} = \varepsilon_{eff} \cdot \sigma \cdot \left(T_p^4 - T_{sky}^4\right)$$

$$= \varepsilon_{eff} \cdot \sigma \cdot \left(T_p + T_{sky}\right) \cdot \left(T_p^2 + T_{sky}^2\right) \cdot \left(T_p - T_{sky}\right)$$

$$\approx U_R \cdot \left(T_p - T_{sky}\right) \tag{8}$$

The latter assumption can be made since the term $\sigma \cdot (T_p + T_{sky}) \cdot (T_p^2 + T_{sky}^2)$ is almost constant in the relevant temperature range.

Following a common approach, the convective heat transfer coefficients are assumed to increase linear with the wind speed.

$$\dot{q}_{conv} = \left(U_{c0} + U_{c1} \cdot v_W\right) \cdot \left(T_p - T_a\right)$$

$$= U_c \cdot \left(T_p - T_a\right) \tag{9}$$

It has to be considered that the absorber surface temperature may be above as well as below the ambient temperature. To be able to distinguish between areas with convective gains and losses a "convection factor" $0 \le f_{conv} \le 1$ is introduced. f_{conv} describes the part of the absorber which is colder than the ambient temperature which leads to power gains, cf. fig. 1.

$$f_{conv} := \frac{\min\!\left[T_{p,o}; \max\!\left(T_a; T_{p,i}\right)\right] - T_{p,i}}{T_{p,o} - T_{p,i}} \tag{10}$$

For the usual case $T_a < T_{p,i}$ eq. (10) leads to $f_{conv} = 0$. The effective absorber temperature T_p^+ of the share of the absorber surface with convective power gains can then be described by

$$T_p^+ = T_{p,i} + \left(T_p - T_{p,i}\right) \cdot f_{conv} \; . \tag{11}$$

and analogous T_p^- for the convective losses can be determined by

$$T_p^- = T_{p,o} + \left(T_p - T_{p,o}\right) \cdot \left(1 - f_{conv}\right). \tag{12}$$

The convective heat transfer can then be modelled as

$$\dot{q}_{conv} = \dot{q}_{conv}^+ + \dot{q}_{conv}^- \tag{13}$$

with

$$\dot{q}_{conv}^+ = U_c^+ \cdot \left(T_p^+ - T_a\right) \cdot f_{conv}$$

$$= \left(U_{c0}^+ + U_{c1}^+ \cdot v_W\right) \cdot f_{conv} \tag{14}$$

$$\left[T_{p,i} + \left(T_p - T_{p,i}\right) \cdot f_{conv} - T_a\right]$$

$$\dot{q}_{conv}^- = U_c^- \cdot \left(T_p^- - T_a\right) \cdot \left(1 - f_{conv}\right)$$

$$= \left(U_{c0}^- + U_{c1}^- \cdot v_W\right) \cdot \left(1 - f_{conv}\right) \tag{15}$$

$$\left[T_{p,o} + \left(T_p - T_{p,o}\right) \cdot \left(1 - f_{conv}\right) - T_a\right]$$
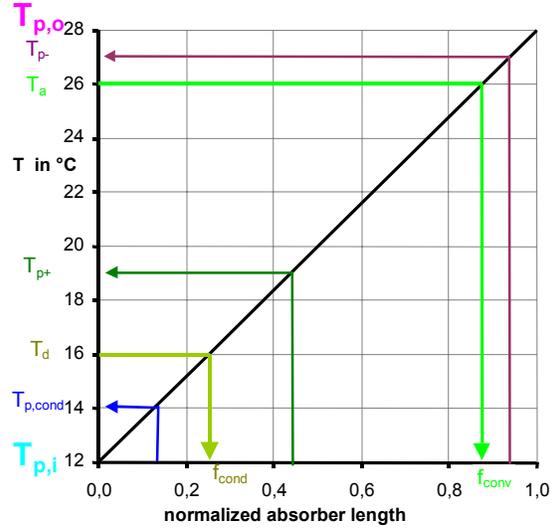

Fig. 1: Depending on the boundary conditions, three different heat transfer mechanism can take place on different areas of the absorber between fluid inlet ($T_{p,i}$) and outlet ($T_{p,o}$). 1.) in the absorber area with a surface temperature T_p beneath the dew point temperature T_d (0 to f_{cond}) due to condensing air humidity, 2.) for $T_p < T_a$ (0 to f_{conv}) convective heat gains and 3.) for $T_a < T_p$ (1-f_{conv} to 1) convective heat losses. Effective, average absorber temperatures for the single heat transfer mechanism can be determined with the assumption of a linear increase of the surface temperature in fluid flow direction.

Following (Soltau 1989), the condensation heat flux can be determined by

$$\dot{q}_{cond} = f \cdot \left[p_s(T_p) - p_s(T_d)\right] \; , \tag{16}$$

where f is a function of the mass transfer coefficient and of the specific evaporation enthalpy. Following (Baehr 1993), the temperature-dependent saturated vapour pressure of water can be described by:

$$p_s(T) = 10^2 \cdot \exp\!\left(19{,}016 - \frac{4064{,}95}{T/°C + 236{,}25}\right) Pa \tag{17}$$

The problem is now to linearize the partial pressure differences in eq. (17) and to convert these into

temperature differences, conforming to the model. For this purpose, the approach was made of building a matrix of coefficients containing the linearized slopes S of the vapour pressure curve for different $T_{p,i}$ and $\Delta T = \max[T_{pi}; \min(T_d; T_{p,o})] - T_{p,i}$.

After the introduction of a condensation factor and an average absorber surface temperature for the condensation heat transfer, similar to eqs. (10) and (11) for the convection,

$$f_{cond} := \frac{\min[T_{p,o}; \max(T_d; T_{p,i})] - T_{p,i}}{T_{p,o} - T_{p,i}} \qquad (18)$$

$$T_{p,cond} = T_{p,i} + (T_p - T_{p,i}) \cdot f_{cond} \qquad (19)$$

and with the assumption of nearly constant water vapour characteristics in the considered temperature interval, eq. (16) passes into

$$\dot{q}_{cond} = U_D \cdot S \cdot (T_{p,cond} - T_d) \cdot f_{cond} \qquad (20)$$

U_D can be determined by parameter fits. Under certain assumptions, cf. (Krämer 1999), U_D can be coupled with the convective heat transfer coefficient U_c (Krämer 1999):

$$U_D = 1{,}78 \cdot 10^{-2} \frac{K}{Pa} \cdot U_c^+ \quad . \qquad (21)$$

With the latter procedure one parameter less has to be determined with the model.

Substituting eqs. (5, 8, 14, 15, 20) in eq. (3) leads to

$$\dot{q}_{use} + U_b \cdot (T_f - T_a) + c_{eff} \cdot \frac{dT_f}{dt}$$
$$= h_i \cdot (T_p - T_f)$$
$$= \dot{q}_{abs} - U_R \cdot (T_p - T_{sky}) \qquad (22)$$
$$\quad - U_c^+ \cdot (T_p^+ - T_a) \cdot f_{conv}$$
$$\quad - U_c^- \cdot (T_p^- - T_a) \cdot (1 - f_{conv})$$
$$\quad - U_D \cdot S \cdot (T_{p,cond} - T_d) \cdot f_{cond}$$

By adding temperature differences in a suitable way the right hand part of eq. (22) can be transformed into

$$h_i \cdot (T_p - T_f) = \dot{q}_{abs}$$
$$\quad - U_R \cdot [(T_p - T_f) + (T_f - T_{sky})]$$
$$\quad - U_c^+ \cdot [(T_p - T_f) + (T_f^+ - T_a)] \cdot f_{conv} \qquad (23)$$
$$\quad - U_c^- \cdot [(T_p - T_f) + (T_f^- - T_a)] \cdot (1 - f_{conv})$$
$$\quad - U_D \cdot S \cdot [(T_p - T_f) + (T_{f,cond} - T_d)] \cdot f_{cond}$$

which can be solved to T_p-T_f and substituted in eq. (22). Applying eq. (9) finally leads to

$$\dot{q}_{use} + U_b(T_f - T_a) + c_{eff} \frac{dT_f}{dt} =$$

$$F^* \cdot \left\{ \begin{array}{l} K_{\alpha,b}(\theta,\gamma_s')\alpha_\perp G_{b,T} + K_{\alpha,d}\,\alpha_\perp\,G_{d,T} \\[4pt] - \varepsilon_{eff} \cdot U_R' \cdot (T_f - T_{sky}) \\[4pt] - (U_{c0}^+ + U_{c1}^+ \cdot v_w) \cdot f_{conv} \\[4pt] \quad [T_i + (T_f - T_i) \cdot f_{conv} - T_a] \\[4pt] - (U_{c0}^- + U_{c1}^- \cdot v_w) \cdot (1 - f_{conv}) \\[4pt] \quad [T_o + (T_f - T_o) \cdot (1 - f_{conv}) - T_a] \\[4pt] - U_D\,S\,[T_i + (T_f - T_i) \cdot f_{cond} - T_d]\,f_{cond} \end{array} \right\} \qquad (24)$$

with

$$F^* = \frac{h_i}{h_i + U_R + U_c^+ f_{conv} + U_c^- (1 - f_{conv}) + U_D\,S\,f_{cond}}$$

F^* is equivalent to the well known collector efficiency factor F'. However, regarding uncovered collectors the back side heat losses are related to the fluid instead of the surface temperature, cf. eq. (3).

As a result, eq. (24) contains the measuring quantities $\dot{q}_{use}, T_f, T_a, G_{bT}, G_{dT}, T_{sky}, v_w, T_i, T_o$ and T_d, furthermore quantities which can be derived by the measured data, material properties or constants like $dT_f / dt, U_R', f_{conv}, f_{cond}, S$ and furthermore the collector model parameters as $F^* K_{\alpha,b}(\theta, \gamma_s'), \alpha_\perp,$ $F^* K_{\alpha,d}, F^* U_R', F^* U_D, F^* U_{c0}^+, F^* U_{c1}^+, F^* U_{c0}^-, F^* U_{c1}^-, h_i,$ U_b and c_{eff}. Some of the parameters can be determined theoretically (e.g. the K 's) whereas the heat transfer coefficients have to be found out by experiments with multi linear regressions of the measured time series (Perers 1993). In principle, eq. (24) would have to be solved iteratively, because f_{conv}, f_{cond} and S can only be determined by evaluating the useful power gain

$$T_{p,*} = T_{f,*} + \frac{\dot{q}_{use}}{h_i} \qquad (25)$$

which is unknown. Furthermore, the time dependency of the fluid temperature would have to be known for the consideration of the effective heat capacity. However, investigations showed that a determination of the absorber surface temperatures with measured values of $\dot{q}_{use}$ in eq. (25) delivers de facto the same parameter values, compared to an iterative application of eq. (24) and (25).

However, if eq. (24) shall be applied for a prediction of solar energy yields, for $f_{conv} < 1$ or $f_{cond} > 0$ an iterative evaluation of $\dot{q}_{use}$ is necessary.
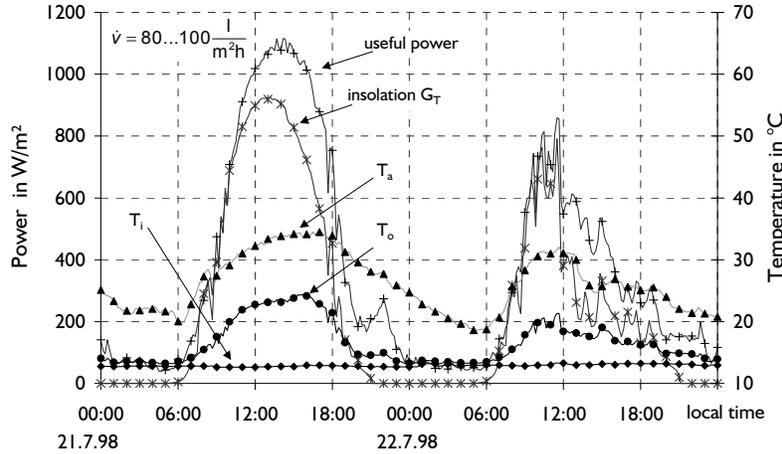
Fig. 2: Exemplary temperature courses and power measured at the uncovered collector. During those days the collector was driven with relatively high specific flow rates, thus the collector outlet temperature remained below the ambient temperature.

3. MEASUREMENTS

In Bishkek (Kyrgyzstan) measurements were carried out for a period of two months. Data have been recorded as one minute average values of the hemispherical-, diffuse- and long wave irradiance, flow-, return- and ambient temperature, absorber flow rate, air humidity and wind speed.

The absorber inlet temperature was between 12° and 13°C, the ambient temperatures in the range of 20° to 35°C. Thus, in most cases the ambient temperature even exceeded the collector outlet temperature. Sometimes the dew point temperature was above the fluid inlet temperature which led to condensation of air humidity at least on a part of the collector.

The average difference between average fluid and ambient temperature was nearly –9 K which led to collector efficiencies, only defined with respect to the incoming irradiance, of higher than one, cf. fig. 2.

4. COMPARISON TO MEASURED DATA

In the evaluation of the experiments two small neglects are included. Firstly, the thermal gains of the flow- and return pipes as well as the distribution and collecting pipes of the collector have not been taken into consideration. An estimation delivered a value of maximal 10 W/m² for these effects. Secondly, as the distributing and collecting pipes of the absorber were installed beside each other, a reduction of the aperture area due to the turn loops of the absorber strips appeared. On the other hand, the collector aperture area was complemented by additional bridges between the absorber webs. Both reversal effects are nearly in the same order of a few percent of the collector aperture area.

(Hilmer 1996) derived a two axis incident angle modifier function $K_{\alpha,b}(\theta,\gamma'_s)$ numerically as well as $K_{\alpha,d}$ for an absorber which was geometrically nearly identical. These functions were used for the determination of $\dot{q}_{abs}$ in eq. (24).

The determination of all remaining parameters in eq. (24), which are $\alpha_\perp$, h_i, U^+_{c0}, U^+_{c1}, U^-_{c0}, U^-_{c1}, U_b, ε_{eff} and c_{eff}, by multi linear regression with the entire data set of nearly 7500 10-minute mean values failed.

For U_b (< 0) as well as for $\alpha_\perp$ and ε_{eff} (both values > 1) no physical sensible values could be determined. Also h_i was overestimated significantly. Thus, the model equation (24) has to be further restricted.

During the measured period, convective heat losses could be observed only at quite a few data sets with very low specific flow rates ($\dot{v} \leq 20$ l/m²h). Under these conditions the model assumption of a linearly increasing fluid temperature in the absorber is not valid any more. Thus, only data sequences with flow rates between 40 and 120 l/m²h and hereby without convective losses (always f_{conv}=1) have been taken into account in the following evaluations.

The back side of the absorber is in thermal contact with the bearing area. The roof, however, consisted of a complicated construction made of asphaltic felt, concrete and wood. Hereby it was not possible to determine a representative roof temperature for the heat exchange with the absorber. Furthermore, beneath parts of the absorber frequently condensate could be observed. A mathematical modelling of condensation and evaporation processes between roof and absorber appear to be difficult. The back side of the absorber was assumed to be adiabatic with U_b=0.

The heat transfer coefficient h_i from the absorber surface to the fluid is dominated by heat conduction in the absorber material and was numerically determined by (Schmidt 1999) with the use of the CFD-program Fluent. For laminar flow a value of h_i = 200 W/m²K was found, for turbulent flow h_i = 290 W/m²K, both values with respect to the collector aperture area. Sensitivity analysis showed that the value of h_i has only small influence on the other collector parameters determined.

A renewed parameter fit with the remaining parameters $\alpha_\perp$, U^+_{c0}, U^+_{c1}, ε_{eff} und c_{eff} resulted in mostly sensible values, only $\alpha_\perp$ =1.01 was out of the ordinary. Probably a net heat flux to the absorber takes place from

the roof covering, as mentioned made of black asphaltic felt. For the effective emission coefficient of the absorber a weak minimum for ε_{eff} =0.73 could be determined. A data analysis showed that the values of $\alpha_\perp$ and ε_{eff} are strongly correlated. Surprisingly, ε_{eff} is no sensitive parameter for the overall result. A proper explanation might be that the sky temperature T_{sky} very often was between the absorber surface temperatures at the fluid inlet and outlet, thus the net heat exchange between absorber and sky by infrared radiation was only poor.

The effective heat capacity c_{eff} was determined about twice as high as theoretically expected. Due to the stable weather conditions during the experiments variations of c_{eff} have nearly no influence on the overall result as well.

U_{c0}^+ and U_{c1}^+ were determined to be 2.8 W/m²K and 7.0 (W/m²K)/(m/s), respectively, which is in the expected range. However, also these parameters are highly correlated. During the measurements only seldom higher wind speed was observed, furthermore the used anemometer had a starting velocity of about 1 m/s.

Energetically, the condensation did not make a big difference. If U_D remains in the model as a free parameter, cf. eq. (24), the share of q_{cond} on q_{use} was in the range of 2 %. If U_D is coupled with U_{c0}^+, eq. (21), the share of q_{cond} is about 1 %. In the latter case the condensation heat transfer coefficient is almost entirely dominated by the convective heat transfer coefficient which is about forty times more relevant regarding q_{use}. In the framework of the evaluated experiments it could not be determined which approach should be preferred. However, obviously $\dot{q}_{cond}$ was strongly overestimated if U_c^+ in eq. (21) was substituted not only by U_{c0}^+, but also by the wind speed proportional coefficient $U_{c1}^+ \cdot v_w$.

The developed model is able to reproduce the measured collector gains for clear and for cloudy periods very well, the differences between measured and modelled power gains are nearly always within the interval of measurement precision, cf. fig. 3. For typical collector gains of 6 to 12 kWh/m²d, the average deviation of the daily sums of the collector gains are below 5%, for the entire period below 1%.

The restrictions mentioned above regarding not determinable parameters do not make the model approach uncertain, but are caused by the specific and hardly influenced boundary conditions during the in-situ measurements.

5. SUMMARY

A model was developed to describe the thermal behaviour of uncovered collectors. The model covers different heat transfer coefficients of convection and condensation which can lead to heat gains and losses on different sections of the absorber surface. Thus, the shares of the single quantities of heat contributed by different heat transfer paths can be determined. Main model assumption is a linear increase of the absorber surface temperature in direction of the fluid flow, thus the application is limited to sufficiently high flow rates.

The results of the model have been compared with data measured at an uncovered collector of 50 m² for two months. However, due to very low fluid inlet temperatures and high ambient temperatures convective heat losses of the absorber have been observed only seldom and the model could not have been validated complete yet.
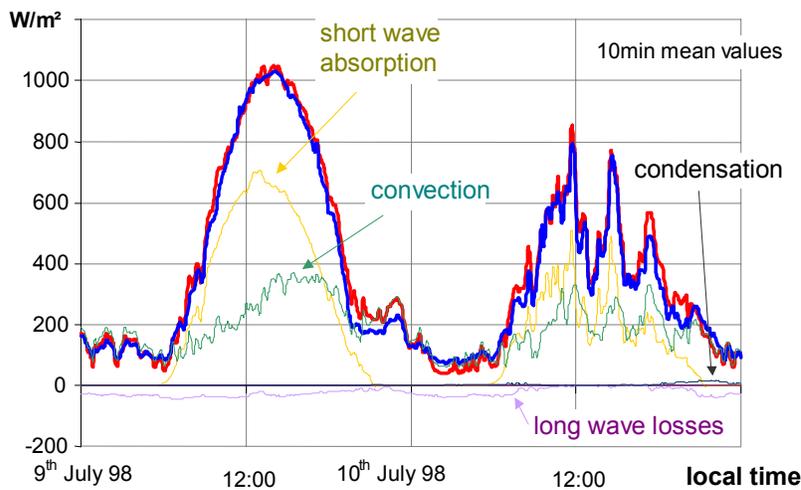

Fig. 3: Comparison of the measured (blue) and modelled (red) collector power gain for two typical measured days. Following the determined parameter and the single terms in eq. (24), the cumulative heat gains due to absorption of solar irradiance have been only 20% higher compared to the convective heat gains.

NOMENCLATURE

All area specific quantities are related to the aperture area of the collector.

c_{eff}	J/m²K	effective heat capacity of the collector
$c_1 \ldots c_6$	different	constants in the model equation of EN 12795 (2001)
E_L	W/m²	long wave irradiance
f_{cond}	-	share of the collector aperture area where condensation takes place
f_{conv}	-	share of the collector aperture area where convective heat gains take place
F^*	-	uncovered collector efficiency factor
F'	-	collector efficiency factor
G_T	W/m²	hemispherical radiation in the collector plane
G_{bT}	W/m²	hemispherical beam radiation in the collector plane
G_{dT}	W/m²	hemispherical diffuse radiation in the collector plane
h_i	W/m²K	heat transfer coefficient between collector surface and fluid
$K_{\alpha,b}$	-	incident angle modifier function for beam radiation
$K_{\alpha,d}$	-	incident angle modifier constant for diffuse radiation
p_s	Pa	saturated vapour pressure of water
$\dot{q}_{abs}$	W/m²	heat flux by short wave radiation
$\dot{q}_b$	W/m²	back side heat flux from or to the absorber
$\dot{q}_{conv}$	W/m²	convective heat flux
$\dot{q}_{conv}^+$	W/m²	convective power gains
$\dot{q}_{conv}^-$	W/m²	convective power losses
$\dot{q}_{cond}$	W/m²	heat flux by condensation
q_{cond}	W/m²	heat gain by condensation
$\dot{q}_{sky}$	W/m²	heat flux by long wave radiation
$\dot{q}_{use}$	W/m²	useful power gain
q_{use}	Wh/m²	useful energy gain
S	K/Pa	approximated slope of the linearized saturated vapour pressure curve
T_a	°C	ambient temperature
T_d	°C	dew point temperature
T_f	°C	average fluid temperature = $(T_i+T_o)/2$
T_i	°C	inlet temperature of the absorber
T_o	°C	outlet temperature of the absorber
T_p	°C	average absorber surface temperature = $(T_{p,i}+T_{p,o})/2$
$T_{p,i}$	°C	absorber surface temperature at the fluid inlet
$T_{p,o}$	°C	absorber surface temperature at the fluid outlet
T_p^+	°C	average temperature of the share of the absorber surface with convective heat gains
T_p^-	°C	average temperature of the share of the absorber surface with convective heat losses
$T_{p,cond}$	°C	average temperature of the share of the absorber surface where condensation takes place
T_{sky}	K	sky temperature, equivalent to the black body radiation from the sky
U_b	W/m²K	heat transfer coefficient on the back side of the absorber
U_D	W/m²K	condensation heat transfer coefficient
U_c	W/m²K	convection heat transfer coefficient
U_{c0}	W/m²K	wind independent part of the convection heat transfer coefficient
U_{c1}	Ws/m³K	wind dependent part of the convection heat transfer coefficient
U_c^+	W/m²K	heat transfer coefficient for convective gains
U_c^-	W/m²K	heat transfer coefficient for convective losses
U_R	W/m²K	heat transfer coefficient for long wave radiation
U_R'	W/m²K	:= U_R / ε_{eff}
v_w	m/s	wind speed in the collector plane
$\dot{v}$	l/m²h	specific flow rate
$\alpha_\perp$	-	absorption coefficient at normal incident
ε_{eff}	-	effective emission coefficient of the absorber surface
γ_s', θ	°	incident angles of the beam radiation
ρ	kg/m³	density
σ	W/m²K⁴	Stefan-Boltzmann constant

LITERATURE

Baehr, H.D. (1993): Thermodynamik, *Springer Verlag* Berlin, 8. Auflage

Hilmer, F. (1996): Modellierung des Betriebsverhaltens nicht abgedeckter Sonnenkollektoren bei zeitlich veränderlichem Fluidstrom, *Dissertation*, Universität Marburg

ISO 9806-3 (1995): Test Methods for Solar Collectors – Part 3: Thermal Performance of Unglazed Liquid Heating Collectors (Sensible Heat Transfer only) Including Pressure Drop

Krämer, M. (1999) Untersuchung des Einsatzes unabgedeckter Kollektoren zur Vorerwärmung von Frischwasser im Fernwärmenetz Bischkek (Kirgisien), *Diplomarbeit*, Universität Marburg, FB Physik

Perers, B. (1987): Performance Testing of Unglazed Collectors, *Report for IEA Task III*, Studsvik Energy, Sweden

Perers, B. (1993) Dynamic Method for Solar Collector Array Testing and Evaluation with Standard Database and Simulation Programs, *Solar Energy 50,* 6, pp. 517-526

EN 12975-2 (2001), Thermal Solar Systems - Collectors - Part 2: Test methods

Schmidt, R. (1999): personal talk, Braunschweig Technical University

Soltau, H. (1989): Das thermische Verhalten offener Kollektoren, *VDI-Verlag* Düsseldorf

Vajen, K., Krämer, M., Orths, R., Boronbaev, E.K. (1999) Solar Absorber System for Preheating Feeding Water for District Heating Nets, *Proc. ISES Solar World Congress*, 4.-9.7.1999, Jerusalem, Vol III, pp. 90-91

ACKNOWLEDGEMENTS